Organellomics: AI-driven deep organellar phenotyping of human neurons

Lena Molitor[1,2*], Sagy Krispin[1,2*], Welmoed van Zuiden[1,2], Yehuda M. Danino[1,2], Noam Rudberg[1,2], Chen Bar[1,2], Emmanuel Amzallag[1,2], Jazz Lubliner[1,2], Aviad Siany[1,2], Chen Eitan[1,2], Yahel Cohen[1,2], Nancy S. Yacovzada[1,2#], Eran Hornstein[1,2$]

[1]Department of Molecular Genetics, Weizmann Institute of Science,

[2]Department of Molecular Neuroscience, Weizmann Institute of Science

* These authors contributed equally

Corresponding Author for machine learning: Nancyy@weizmann.ac.il

$ Corresponding Author for all other facets of the work: Eran.Hornstein@weizmann.ac.il

Abstract

Systematic assessment of organelle architectures in cells, known as the organellome, could provide valuable insights into cellular states and disease pathologies but remains largely uncharted. Here, we devised a novel pipeline combining self-supervised deep learning and transfer learning to generate a Neuronal Organellomics Vision Atlas (NOVA). Analyzing over 1.5 million confocal images of 24 distinct membrane-bound and membrane-less organelles in human neurons, we enable a simultaneous evaluation of all organelles. We show that organellomics allows the study of cellular phenotypes by quantifying the localization and morphological properties embodied in multiple different organelles, using a unified score. We further developed a strategy to superimpose all organelles, which represents a new realization of cellular state. The value of our approach is demonstrated by characterizing specific organellar responses of human neurons to stress, cytoplasmic mislocalization of TDP-43, or disease-associated variations in ALS genes. Therefore, organellomics offers a novel approach to study the neuro-cellular biology of diseases.

Highlights

AI-driven organellomics without cell segmentation or multiplexed imaging.

Analysis of 24 membrane-bound and membrane-less organelles in more than 1.5 million images of human neurons.

Quantitative organelle-level description of neuronal response to chemical and genetic perturbations.

Organelles ranked on a single metric scale and integrated organellome view via superposition of multiple organelles.

Keywords: AI, computer vision, deep learning, machine learning, self-supervised learning, variational autoencoder, neurons, neurodegeneration, subcellular architecture, organelles, biomolecular condensates, inter-organellar interdependency.

Introduction

Organellomics, the systematic study of subcellular organellar architecture (the organellome), may be a useful strategy to directly phenotype cells by their subcellular compartments. This is conceivable since the quantification of RNAs, lipids, metabolites and proteins that compose organelles cannot be directly translated into complex organelle properties. Furthermore, organelles are interconnected by functional crosstalk and inter-organelle interdependency (Gottschling and Nyström 2017; Zung and Schuldiner 2020), further supporting the value of organellomics-level insights for cell biology.

The analysis of multiple organelles poses substantial challenges because of the variety of localizations and morphologies, which need to be integrated and evaluated in parallel. Systematic quantification and global evaluation of subcellular architecture has been developed using mass spectrometry-based approaches (Itzhak et al. 2017; Borner 2020; Schessner et al. 2023; Itzhak, Schessner, and Borner 2019; Thul et al. 2017). These do not provide insight about organellar morphology and depend on tedious organelle fractionation, which is limited to only a subset of the organelles. In addition, imaging-based approaches were developed (Kobayashi et al. 2022; Spitzer et al. 2023; Carpenter et al. 2006; Heinrich et al. 2021; Lu et al. 2019; Husain et al. 2023; Long, Yang, and Shen 2020). However, these are largely in non-polarized cultured cells.

Additionally, the study of cellular organization has been traditionally focused on membrane-restricted organelles, such as the nucleus and mitochondria. However, in recent years, certain biomolecular condensates have been identified as membrane-less organelles with specialized functions (Hirose et al. 2022; Banani et al. 2017; Brangwynne 2013; Lyon, Peeples, and Rosen 2021; Alberti and Hyman 2021). Therefore, the study of both membrane-restricted and membrane-less organelles is important for gaining a comprehensive view of cellular biology.

Accordingly, dysfunction of organelles is a central driver of disease. Disorders of membrane-bound organelles such as mitochondria, lysosomes, or autophagosomes have been comprehensively characterized and are associated with distinctive clinical pictures (Platt et al. 2018; Cox and Cachón-González 2012; Gorman et al. 2016; Schapira 2006; Levine and Kroemer 2008; Mizushima and Levine 2020). In addition, compelling evidence suggests a role for membrane-less organellar dysfunction in neurodegeneration (Nedelsky and Taylor 2019; Alberti and Dormann 2019; Alberti and Hyman 2021).

We hypothesized that comprehensively capturing the localization and morphological patterns across the entire organellome will allow inference about the relationships between different organelles and shed light on inter-organellar biology in disease phenotypes. To test this hypothesis, we employed an image representation learning approach, particularly based on deep variational autoencoders, which allows the capturing of high-level abstraction of morphological features from immunofluorescent confocal images (Long, Yang, and Shen 2020; F. Wang and Wei 2022; Kobayashi et al. 2022; Thul et al. 2017; Cho et al. 2022). Widely used approaches to extract features from images require a-priori assumptions about objects to be studied (Bray et al. 2016; Stirling et al. 2021). However, deep representation learning enables automatic feature extraction, which is unbiased and does not require a pre-defined object or task, hence can describe any localization pattern in the image.

Here, we introduce a **N**euronal **O**rganellomics **V**ision **A**tlas (NOVA), a systematic and unbiased organellomics approach that is based on a self-supervised Vector Quantized Variational AutoEncoder

technique (VQ-VAE-2, (van den Oord, Vinyals, and Kavukcuoglu 2017; Razavi, van den Oord, and Vinyals 2019)). NOVA takes as input immunofluorescence images of a panel of cellular organelles in cultured cells, and encodes for subcellular localization patterns. NOVA builds on "Cytoself", a model trained on massive amounts of OpenCell data (Cho et al. 2022; Kobayashi et al. 2022). We applied transfer learning on the pre-trained Cytoself model for generalization and compatibility with highly polarized human neuronal cells. NOVA does not require detection of the cellular borders (segmentation), overcoming a limitation in neuron image analysis (Kim, Son, and Palmore 2015; Ascoli, Donohue, and Halavi 2007; Oberlaender et al. 2007). Furthermore, we associate organelles with unique spectral signatures that enable capturing neuronal cellular states and variable genetic backgrounds. We further developed "synthetic superposition", an *in-silico* technique for integrating the organelle-level data to detect subtle differences in cellular architecture that are not observable by examining a single organelle.

Organellomics reveals the heterogeneity of cell types and conditions and is sensitive enough to depict organellome changes associated with single nucleotide genetic variants. As such, it can be broadly utilized to provide the foundations for a powerful diagnostic avenue in the future.

Results

A deep learning-based model distinguishes different cellular states

The complexity of the organellome in highly polarized cells, like neurons, necessitates a strategy that transforms microscopic images into unbiased, quantitative data. Deep variational autoencoders are generative AI algorithms, successful in encoding images into meaningful features that enable multi-level (hierarchical) latent space representation. To analyze organellar morphology and localization features (referred to here as topography), we employed Cytoself, a self-supervised model for subcellular localization patterns from microscopy images (Kobayashi et al. 2022). We first trained an in-house Cytoself model using the Pytorch framework on the entire dataset of 1,311 proteins in 1,134,592 OpenCell image tiles of human embryonic kidney (HEK293T) cells that were cultured in basal growth conditions (Cho et al. 2022)**, Supplementary Figure 1A**). Cytoself is based on the VQ-VAE-2 deep learning architecture: a two-level vector quantized variational autoencoder, which converts an image into global and local numerical representations (**Methods**). The model is trained to find a set of 2,048 abstract features (codewords) that are stored in a codebook, where each codeword captures important morphology and localization properties of images **(Figure 1A**). Then, a unique combination of codewords is used to represent each image (**Supplementary Figure 1B-D**). The comparison of codeword usage between different conditions (phenotypes) provides a means for uncovering quantitative organellar differences. We created means to compare specific properties of subcellular localization patterns by creating uniform manifold approximation and projection (UMAP) of the representations and by histograms of codeword frequencies, or feature spectra, following (Kobayashi et al. 2022) (**Figure 1A, Supplementary Figure 2B,C, Methods**). Differential feature spectra analysis further enables comparison of organellar topographies and phenotypes (**Supplementary Figure 2D,** see **Methods**).

First, we evaluated whether Cytoself could be extended beyond its initial training to effectively discern cellular states in other cell lines (**Figure 1**, **Supplementary Figure 1B-D**). Thus, we cultured human osteosarcoma (U2OS) cells and induced oxidative stress by sodium arsenite (30 minutes, 0.4 mM, (Protter and Parker 2016; Anderson and Kedersha 2009). Stress granules (SGs), a type of cytoplasmic biomolecular condensate, form in response to stress conditions and are readily identifiable through specific immunostaining of the protein G3BP1 **(Figure 1B)**. However, the actin cytoskeleton or P-bodies (labeled by Phalloidin, or DCP1A, respectively), did not display visually detectable alterations (**Supplementary Figure 2A**). Accordingly, UMAP revealed clear segregation of stressed and unstressed U2OS cell clusters based on stress granule data (G3BP1, adjusted Rand index (ARI), 0.943; **Figure 1B**) and feature spectra, depicted the codeword frequencies.

Although the human eye could not depict the effect of stress on the actin cytoskeleton or P-bodies, the UMAP revealed a moderate degree of separation (**Supplementary Figure 2B,** ARI < 0.6) and feature spectra enables comparison of codewords used to describe the organellar topographies in stress (**Supplementary Figure 2D**).Therefore, Cytoself's performance is robust and works well on a cell type (U2OS), perturbation (stress), and labeling techniques (antibodies and dyes) that were not part of its initial training.

Transfer learning enables detection of subcellular localization patterns in human neurons

While techniques for image analysis of cultured cells are available (Carpenter et al. 2006), automated microscopic analysis of subcellular neuron organization remains extremely challenging. Thus, we next tested whether Cytoself could be applied to induced pluripotent stem cell (iPSC)-derived neurons (Fernandopulle et al. 2018), **Figure 1C**). Images of immune-stained neurons were captured by a spinning disc confocal microscope and subjected to QC and preprocessing steps. Overall, throughout this work we created a comprehensive dataset composed of >1,200,000 image tiles of ~3,300,000 human iPSC-derived neurons (**Supplementary Figure 3A, and Supplementary Materials**).

Upon introduction of sodium arsenite, visible SGs were assembled in neuron images (**Supplementary Figure 1C**). However, Cytoself failed to segregate stressed from unstressed neuron populations based on the stress granule marker G3BP1 (**Figure 1D**, **upper UMAP,** ARI = -0.001). Therefore, Cytoself's training on HEK293T cells was insufficient for the analysis of neurons. To gain applicability to neurons, we applied transfer learning to the Cytoself model (**Methods**, **Figure 1D**). Transfer learning is a machine learning technique where a model developed for one task (Cytoself, protein localization in cancer cells) is reused as the starting point for a model on another task (localization in neurons), leveraging pre-learned patterns to improve performance.
For robustness, data used for training, validation, and test originated from four different batches (~580,000 human iPSC-derived neuron image tiles) while inference was conducted solely on the rest of the batches. The new fine-tuned model was successful in correctly clustering neurons by cellular stress state, using G3BP1 as a marker (**Figure 1D, lower UMAP,** ARI = 0.821). Therefore, the transfer learning into the new NOVA model expands the capabilities to study human neurons.

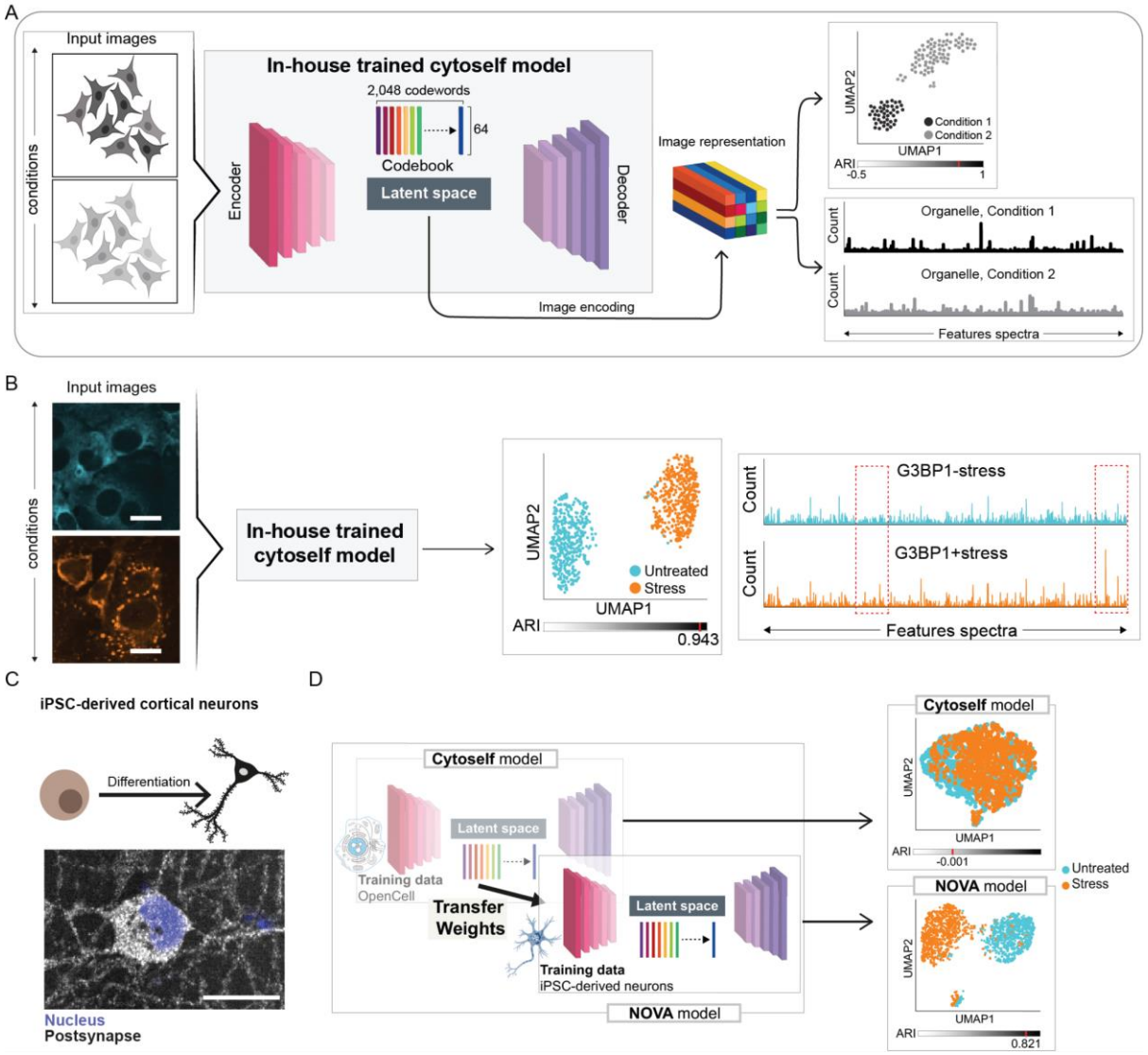

Figure 1: Deep learning-based representation of subcellular localization and morphological patterns in non-polarized and polarized cells. (A) Illustration of the workflow, whereby input images are encoded as features (codewords) in the latent space (Kobayashi et al. 2022). **(B)** Image representations are used for UMAP clustering of U2OS cell topographies in response to sodium arsenite stress, marked by stress granules (G3BP1). Adjusted Rand index (ARI = 0.943). Image representations are also used to create feature spectrum histograms, which display the differential usage of codewords upon stress induction (**Supplementary Figure 1**). Dashed red rectangles depict stress-sensitive regions of the feature spectra, scale bars 20µm. **(C)** iPSC-derived neurons, on day 8 of differentiation. Immunostaining of postsynaptic density protein 95 (PSD95) and nuclear Hoechst 33342 staining, scale bar 20µm. **(D)** Cytoself model fails to cluster iPSC-derived neurons subjected to stress from cultures under basal growth conditions (ARI = -0.001, G3BP1). A transfer learning process on neuronal images established a fine-tuned model termed the NOVA-model, which effectively depicts the response of neurons to stress (ARI = 0.821).

176 **Organellomics: the study of 24 organelles in neurons**

177 To gain a broad organellomic view, we devised a set of 24 key membrane-bound and membrane-less
178 organelles (**Figure 2A**). We stained neurons with specific antibodies that demarcate the 24 organelles
179 (**Table 1**) and captured spinning disc confocal images. The NOVA model allowed encoding of these
180 images and the representations were used to create a UMAP of the full landscape of neuronal
181 organelles (**Figure 2B**). Thus, cluster proximity signifies similarity in either localization or morphology.
182 Notably, two distinct nuclear clusters emerge: one encompasses the nucleus, nucleolus and hnRNP
183 complex and the other features TDP-43 granules, ANXA11 granules, and paraspeckles. These
184 potentially suggest distinctive nuclear substructures. Notably, the proximity of TDP-43 and
185 paraspeckles is consistent with TDP-43 co-localization in paraspeckles (West et al. 2016; Naganuma et
186 al. 2012).
187
188 Next, we analyzed feature spectra, which describe organellar topographies, following the work of
189 (Kobayashi et al. 2022). We hierarchically clustered the feature spectra, and generated ordered
190 feature histograms of each organelle (**Supplementary Figure 1C**). The feature spectra revealed
191 distinctive organellar topographies that could be clustered into 11 groups (clusters, **Figure 2C**).
192 Notable similarities were identified, e.g., between nucleus and hnRNP complex or ANXA11 granules
193 and TDP-43 granules, suggesting similar topographies. In addition, the transport machinery and
194 coated vesicles manifested a shared spectral signal that extended to the presynapse, suggesting
195 coordinated organellar topographies. The 11 clusters were manually aggregated into three families
196 (**Figure 2D**), corresponding to punctate structures, nuclear localized organelles and
197 cytoplasmic/neuritic localized organelles (**Figure 2D, Supplementary Figure 4A**). Taken together,
198 neuronal organellomics with 24 organelles reveals distinct localization or morphology patterns,
199 yielding biologically-interpretable feature spectra and providing insights into neuronal subcellular
200 organization.
201

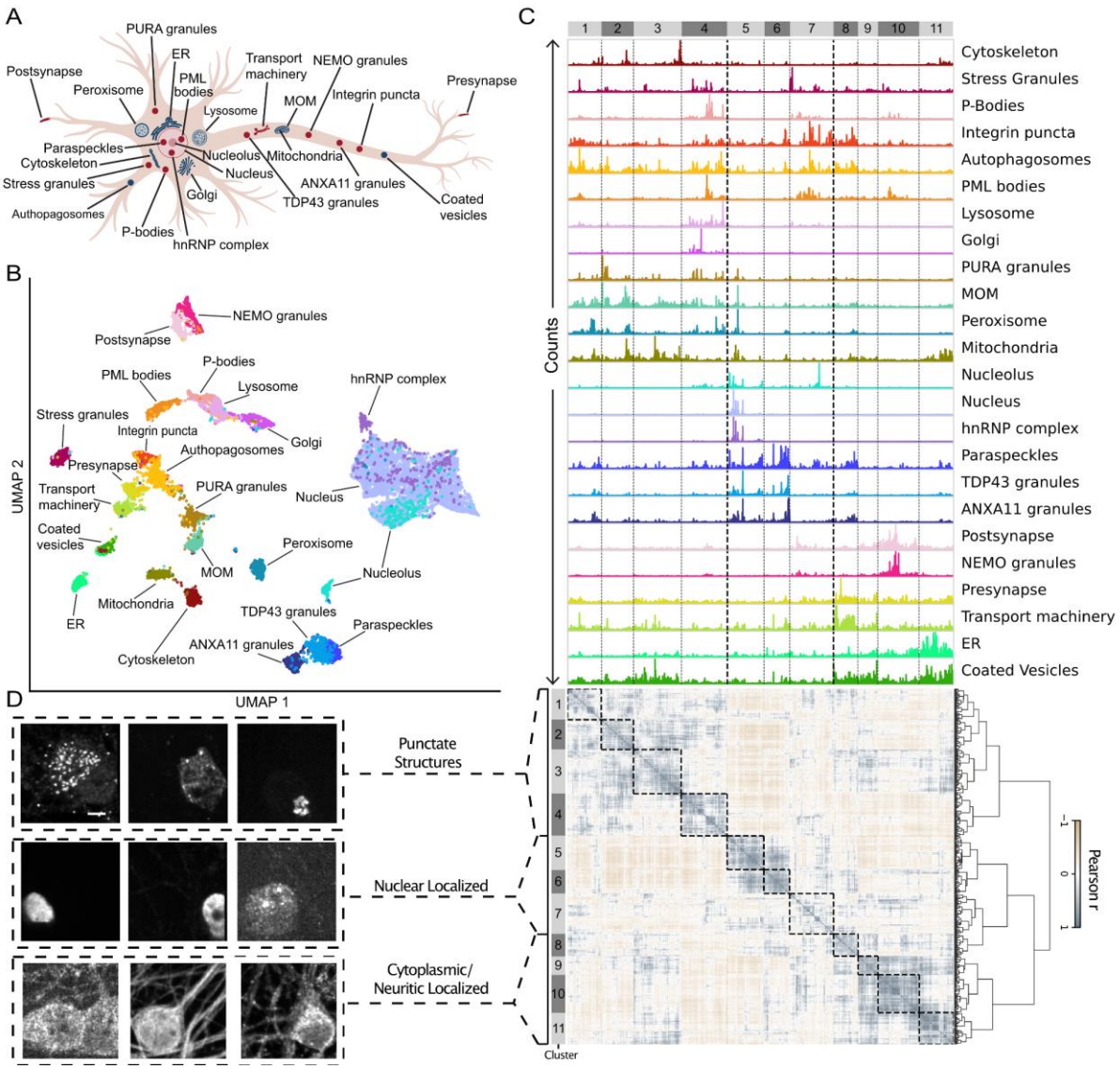

Figure 2: Organellomics reveals distinct topography patterns in neurons. (A) Illustration of the 24 organelles used for the organellomics study. **(B)** UMAP atlas of the neuronal organellome. ARI = 0.357. **(C)** Histogram of features, re-ordered by hierarchical clustering to form a heatmap (Pearson correlation (r)) and feature spectra. Organelle feature spectra are color-coded as in (B). 11 identified clusters can be grouped into three families. **(D)** Representative images displaying the highest utility of the codewords corresponding to specific feature spectra clusters, scale bar 5µm.

214 **Table 1:** 24 key organelles analyzed in this study, and abbreviations used in this manuscript. Selected
215 marker per organelle with relevant literature.

Organelle	Abbreviation	Marker	Relevant Literature
Nucleus		Hoechst 33342	(Chazotte 2011a)
Mitochondria		Mitotracker	(Chazotte 2011b)
Mitochondria Outer Membrane	MOM	TOMM20	(Wurm et al. 2011)
Golgi Apparatus	Golgi	GM130	(Turner et al. 2020)
Endoplasmic Reticulum	ER	Calreticulin	(Nava et al. 2015)
Actin Cytoskeleton	Cytoskeleton	Phalloidin	(Chazotte 2010)
Autophagosomes		SQSTM1	(Kageyama et al. 2021)
Lysosomes		LAMP1	(Gowrishankar, Wu, and Ferguson 2017)
Peroxisomes		PEX14	(Koyano et al. 2019)
Coated Vesicles		CLTC	(Tsygankova and Keen 2019)
Integrin puncta		CD41	(Xiang et al. 2016; Mobarrez et al. 2016)
Nucleolus		NCL	(Srivastava et al. 1989)
Paraspeckles		NONO	(Fox, Bond, and Lamond 2005; Fox et al. 2002)
TDP-43 granules		TDP-43	(Tsuji et al. 2012)
Heterogeneous Nuclear Ribonucleoprotein Complex	hnRNP complex	FUS	(Calvio et al. 1995; Yang et al. 2014)
Promyelocytic Leukaemia Nuclear Bodies	PML bodies	PML	(Weis et al. 1994)
P-Bodies		DCP1A	(Eystathioy et al. 2003)
Stress Granules		G3BP1	(Tourrière et al. 2003)
ANXA11 granules		ANXA11	(Liao et al. 2019)
PURA granules		PURA	(Daigle et al. 2016; Molitor et al.

			2023)
NEMO granules		NEMO	(Du et al. 2022)
Microtubule-Associated Transport Machinery	transport machinery	KIF5A	(Liu et al. 2021)
Presynaptic Terminals	Presynapse	SNCA	(Ray et al. 2020; Bayer et al. 1999)
Post-Synaptic Subcompartments	Postsynapse	PSD95	(Sampedro, Bussineau, and Cotman 1981)

Differential analysis reveals coordination of organellar responses in stressed neurons

Our hypothesis is that capturing localization and morphological patterns across the organellome will shed light on the cellular state. To test this, we first characterized the effect of sodium arsenite stress on the organellome in neurons. UMAP analysis revealed differential localization or morphology patterns of some of the organelles upon stress induction **(Figure 3A).** In stress, both G3BP1 and PURA converge on stress granules (Di Salvio et al. 2015; Daigle et al. 2016; Markmiller et al. 2018)**,** consistent with a significant and coordinated change in their topographies (G3BP1 ARI = 0.821, PURA ARI = 0.718, **Figure 3A**). In addition, PML nuclear bodies displayed altered topography (ARI = 0.756). These results were consistently replicated in three separate batches, and suggest that the most stress-sensitive organelles in neurons are stress granules (ARI = 0.757 or 0.546 for G3BP1 or PURA, respectively), and PML nuclear bodies (ARI = 0.242, **Supplementary Figure 5A)**.

We further developed an orthogonal scoring technique to quantify organellar topographies (organelle scoring) using the full representation (instead of only 2 UMAP components). For this, we calculated the Euclidean distances of the representations and ranked organelles by their ability to discriminate between states (**Figure 3B**, **Methods**). Organelle scoring allows direct comparison of all organelles in neurons under basal and stress conditions. We found substantial alterations in the topography of stress granules (by both G3BP1 and PURA) across eight experimental batches. This was substantiated by an additional independent experimental repeat with six batches, together totaling 14 batches (**Supplementary Figure 5B, C**). Notably, the organelles that were most affected by stress were stress granules and PML nuclear bodies. Reproducible stress-associated changes were also quantified in TDP-43 granules, the mitochondria, integrin puncta, autophagosomes, P-bodies and nucleoli. While changes in stress granules were noticeable by a human experimentalist, all other organellar changes escaped the human eye, emphasizing the value of computer-based analysis. Furthermore, organelle scoring allows for relative comparison of different organelles even at distinct and physically separated cellular compartments (nucleus, cytoplasm) or with very different morphologies.

We compared the performance of the NOVA-model to CellProfiler, an established object-based image analysis technique (Stirling et al. 2021). To this end, we developed a pipeline that extracts 347 CellProfiler features (Stirling et al. 2021)). Organelle ranking on the basis of CellProfiler features in response to neuronal stress revealed changes in PML nuclear bodies, stress granules (PURA) and other organelles that were consistent with the NOVA-model. However, unexpectedly, CellProfiler ranked

250 stress granules (marked by G3BP1) as a mediocre readout of cellular stress **(Supplementary Figure**
251 **5D).** Altogether, the NOVA-model reveals the broad changes neuronal organelles undergo in stress
252 and ranks them on a single scale system. While automatically extracting features, it is comparable or
253 perhaps more sensitive than an object-based approach.
254
255 To uncover coordination in responses between different organelles and identify potential
256 interorganelle regulation we next performed a differential analysis of spectral features in response to
257 stress and utilized it for network graph analysis. We identified four correlating subgroups of organelles
258 (**Figure 3C, Supplementary Figure 5E**). One subgroup included stress granules (PURA and G3BP1), the
259 Golgi apparatus, lysosome and mitochondrial outer membrane (MOM). This analysis suggests an
260 orchestrated stress response across these four organelles. The changes in the differential feature
261 spectra of these organelles are accordingly localized to a particular region of the spectrum (**Figure 3D**).
262 The intriguing correlation of stress granule and mitochondria outer membrane suggests that
263 potentially these organelles display coordinated topographies in response to stress. We provide
264 cursory support for this hypothesis by demonstrating higher colocalization of stress granules and
265 mitochondria in U2OS cells under proteotoxic stress (**Supplementary Figure 5F, G**). In addition, the
266 correlation of differential feature spectra of PML nuclear bodies and P-bodies, or that of nuclear
267 organelles (paraspeckles, TDP-43 granules, nucleoli, and hnRNP granules), suggests mutual behaviors
268 and potential underlying biological coordination (**Figure 3C**). Therefore, organellomics uncovers broad
269 neuronal responses to stress that can be quantified onto a unified scale across organelles.

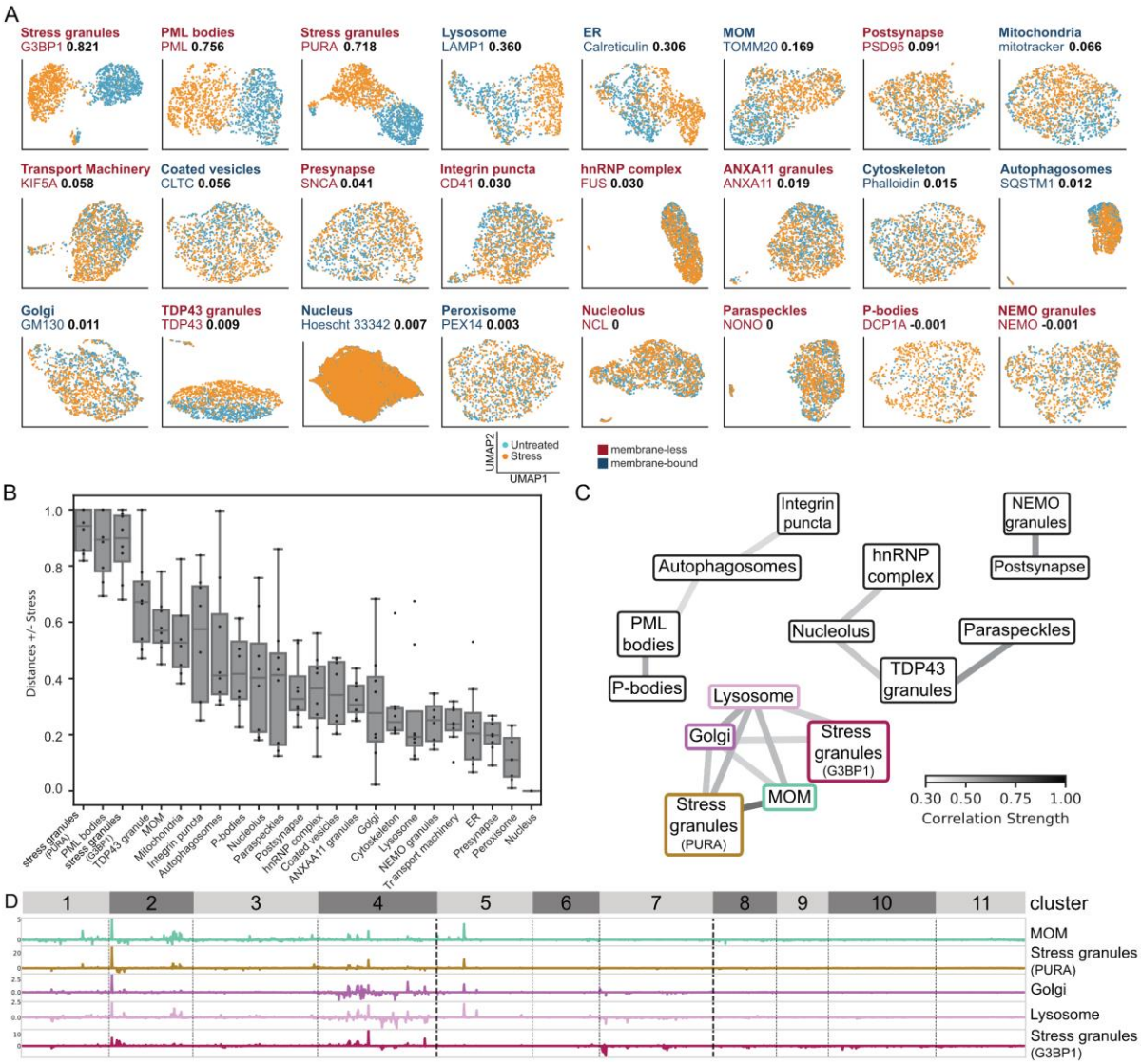

Figure 3: A coordinated neuronal organellar response to stress. (A) UMAPs of 23 organelles in human neurons in response to stress. Stressed (orange) or unstressed (light blue) neurons. Membrane-bound (blue) and membrane-less (red) organelles with the specific marker annotated. ARI (black). Representative data from a single batch. **(B)** Organelle scoring, as box plot and whiskers, via Euclidean distances of organelles topographic patterns in response to stress, using NOVA full latent features across 8 batches. **(C)** A network graph of the correlations of the differential feature spectra for organelles ± stress. Edges depict a Pearson correlation r > 0.4 **(D)** Differential feature spectra (± stress) of selected organelles. Scale varies across organelles (y axis).

Cytoplasmic TDP-43 impacts neuronal organellar dynamics and P-body size

To investigate whether our organellomics approach can generate novel mechanistic insights into disease states, we studied iPSC-derived neurons expressing doxycycline-inducible TDP-43 (TARDBP), which lacks a functional nuclear localization signal (NLS; TDP-43^{deltaNLS}) leading to mislocalization of TDP-43 to the cytoplasm (**Figure 4A, B**). TDP-43 cytoplasmic malpositioning is a hallmark of human neuropathology in amyotrophic lateral sclerosis (ALS) and frontotemporal dementia (FTD,

(Tziortzouda, Van Den Bosch, and Hirth 2021). Accordingly, we created a comprehensive dataset composed of an additional 8 batches, yielding >328,000 image tiles. Four of the batches were used to fine-tune the NOVA-model, and the four remaining image batches were used for inference (**Supplementary Figure 3A, 6A, and Supplementary Materials**). As expected, we observed alterations in TDP-43 granule topography (**Figure 4C**). Organelle scoring of TDP-43 ±Dox reassuringly revealed that the topography of TDP-43 was affected by the cytoplasmic mislocalization of TDP-43 granules (termed TDP-43 granules 1 and 2 when immunostaining with two different N-terminal specific antibodies recognizing amino acids 203-209; one monoclonal and one polyclonal antibody (Tsuji et al. 2012), **Figure 4D, Supplementary Figure 6B, C**). However, P-bodies , hnRNP complex, nucleoli and the Golgi apparatus topographies were also altered. In contrast, no discernible changes were identified in stress granules (ranked 18th and 21st out of 24, G3BP1 and PURA respectively). These findings suggest that the effect of cytoplasmic TDP-43 on the organellome is largely independent of stress granules, aligning with (Gasset-Rosa et al. 2019), who observed that cytosolic TDP-43 assemblies operate separately from conventional stress granules. The strong coordinated response of TDP-43 granules and P-bodies was validated using CellProfiler, which suggests that P-body area decreased upon cytoplasmic TDP-43 induction. However, P-body numbers were unchanged (**Figure 4E**, **Supplementary Figure 6D**). Altogether, cytoplasmic TDP-43 mislocalization impacts several organelles, most notably P-bodies.

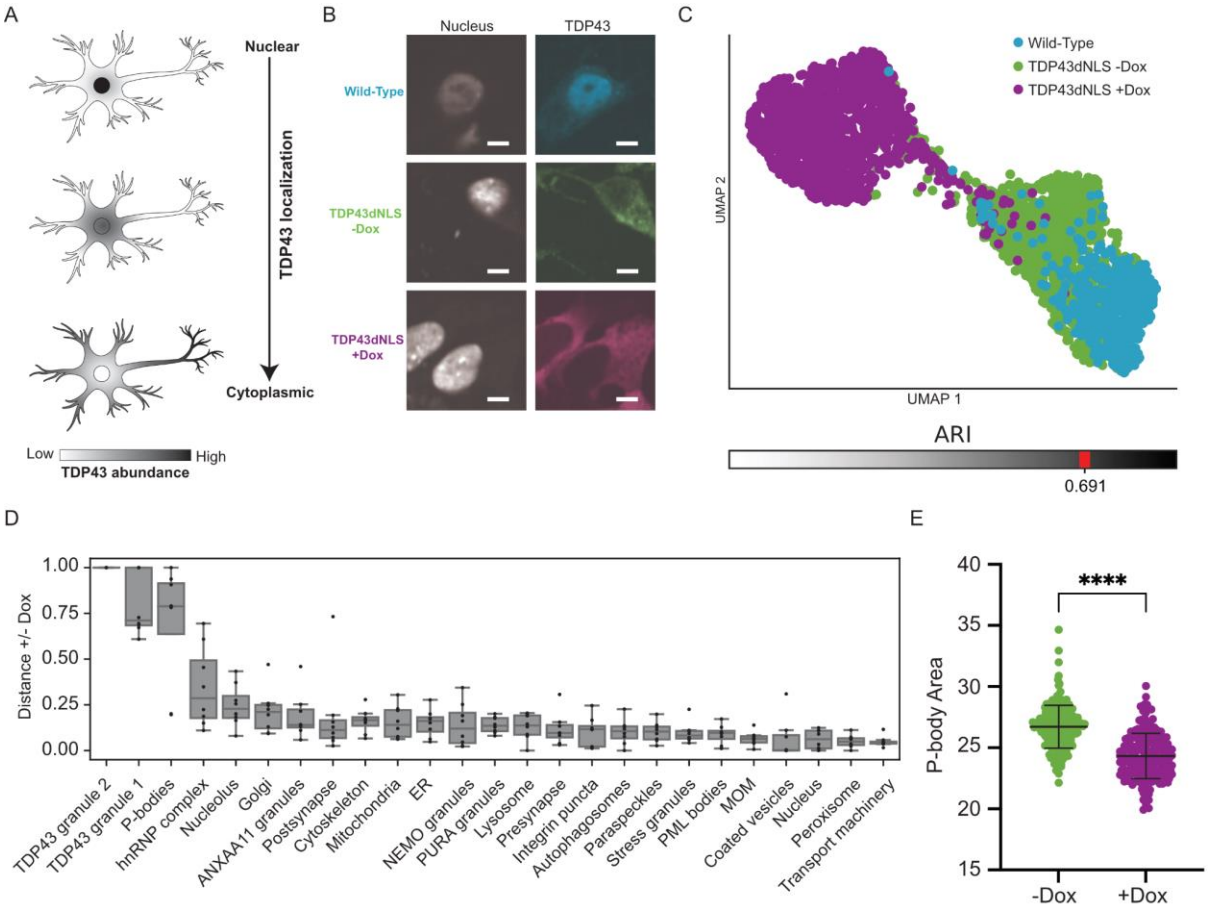

Figure 4: Impact of Cytoplasmic TDP-43 on the Neuronal Organellome. (A) A diagram of the induction of cytoplasmic TDP-43 in human iPSC-derived neurons: wild type, and a clone that overexpresses an inducible form of TDP-43 with a mutated nuclear localization signal (dNLS). Uninduced / doxycycline-

induced expression of TDP-43 (-Dox / +Dox) and **(B)** representative images. Scale bar 5µm. **(C)** UMAP of TDP-43 granules 1 (Proteintech antibody 10782-2-AP) in wild type and TDP-43 (±Dox) cell lines. **(D)** Organelle scoring by distance using the full latent space in 8 batches. TDP-43 granules (1 and 2), were assessed using two independent antibodies (Proteintech 10782-2-AP and 60019-2-Ig, respectively). **(E)** CellProfiler analysis of P-body area ±Dox induced expression of cytoplasmic TDP-43, $p<0.0001$, unpaired two-sided parametric t-test.

Organellomics captures the effect of ALS-associated single-nucleotide variants in neurons

We hypothesized that an integrated organellome view, that takes into account all 24 organelles, can be useful to holistically map cellular states. To address this hypothesis, we developed "synthetic superposition", a novel *in-silico* technique, that combines the representations of all organelles per perturbation (**Figure 5A, Methods**). Synthetic superposition enables a consolidated perspective on the integrated organellome. This is technically gained by randomly selecting an image tile of each of the 24 organelles, encoding them into codeword histograms (2,048 values per organelle), and concatenating these representations (which yields a single vector of 49,152 values). We sought to assess the effect of various perturbations on organellome superposition. The integrated organellome effectively captured the impact on neurons of stress (ARI = 0.893, **Figure 5B**) and of cytoplasmic mislocalization of TDP-43 (ARI = 0.145, **Figure 5C**).

We also asked whether our approach could be used to study organellar dysfunction in the context of amyotrophic lateral sclerosis (ALS), a neurodegenerative disease with a substantial genetic component. For this, we utilized iPSC-derived neurons harboring ALS-associated genetic mutations on a single isogenic background, from the iPSC Neurodegenerative Disease Initiative (iNDI, (Ramos et al. 2021). iNDI lines gained traction as useful tools for research and allow a controlled comparison of different neurodegeneration-associated mutations. We compared the effect of homozygous ALS-associated mutated genes FUS R495*, TDP-43 M337V, OPTN Q398E and TBK1 E696K (Fernandopulle et al. 2018; Ramos et al. 2021) versus the isogenic control line (Wild-type **Figure 5D**). In other models, FUS R495* is depleted from the nucleus and undergoes aberrant phase separation (Hofweber et al. 2018; Yoshizawa et al. 2018; Dormann et al. 2010). Likewise, the TDP-43 M337V mutation disrupts its localization (Zhang et al. 2013; Bilican et al. 2012; Mutihac et al. 2015). Both *TDP-43 M337V* and *OPTN Q398E* alter vesicular trafficking (Feneberg et al. 2020; Qiu et al. 2022). *OPTN Q398E* further alters the secretory pathways, causes Golgi fragmentation, dysregulated autophagosomes and enhances ER stress (Qiu et al. 2022). Finally, *TBK1 E696K* hampers mitophagy and autophagy (Li et al. 2016).

The integrated organellome of the four ALS-associated genetic models and wild-type, superpositioning all 24 organelles, demonstrate the differences between the cell lines and is reproducible across different batches (**Figure 5E**, **Supplementary Figure 7A, B**). *TBK1 E696K and FUS R495** were most different from the wild-type, whereas TDP-43 *M337V* and OPTN *Q398E* remained in the vicinity of the wild-type, suggesting that their organellome is unaffected (**Figure 5E**).

Since the topographical changes associated with *FUS R495** were pronounced, we focused on FUS. The integrated organellome revealed a strong similarity between the heterozygous and homozygous *FUS R495** mutants. Additionally, the revertant (genetically restored) line was distinct from the FUS mutant clusters, yet it still did not reside near the wild-type line (**Figure 5F**). This suggests that the differences between the wild-type and the revertant are not fully recovered.

The hnRNP complex (FUS) analysis reveals FUS mutants' clustering apart from the wild-type and revertant lines. Accordingly, microscopic images reveal that hnRNP complex (FUS) is detected in the cytoplasm of *FUS R495** heterozygous and homozygous mutants and it is constrained to the nucleus in the wild-type and the FUS revertant lines (**Figure 5G, H**). Interestingly, feature spectra of the FUS R495* mutants lines differed from that of the WT and FUS revertant lines (Pearson correlation r = 0.11, 0.08 for FUS homozygous, FUS heterozygous, respectively). Noteworthy, when synthetic superposition was performed by combining all other 23 organelles, omitting the hnRNP complex, the FUS revertant clustered closer to *FUS R495** and apart from the wild-type line (**Supplementary Figure 7C**). Together, these data suggest that the hnRNP complex is the predominant organelle affected by the FUS R495* mutation, which is effectively recovered by genetic correction of the mutation. However additional elements, such as the passage in culture, or CRISPR off targets, make the revertant line dissimilar to the wild-type. Finally, a genetic SNCA E46K mutation that is associated with Parkinson's Disease (PD) was studied. In the integrated organellome, SNCA E46K emerges as another distinct cluster, suggesting that it differs from neurons with ALS-associated mutations (**Supplementary Figure 7D**).

Altogether, our data demonstrate that NOVA is broadly applicable as a tool for image analysis in neuroscience and can facilitate neurodegeneration-focused organellomic studies in human neurons.

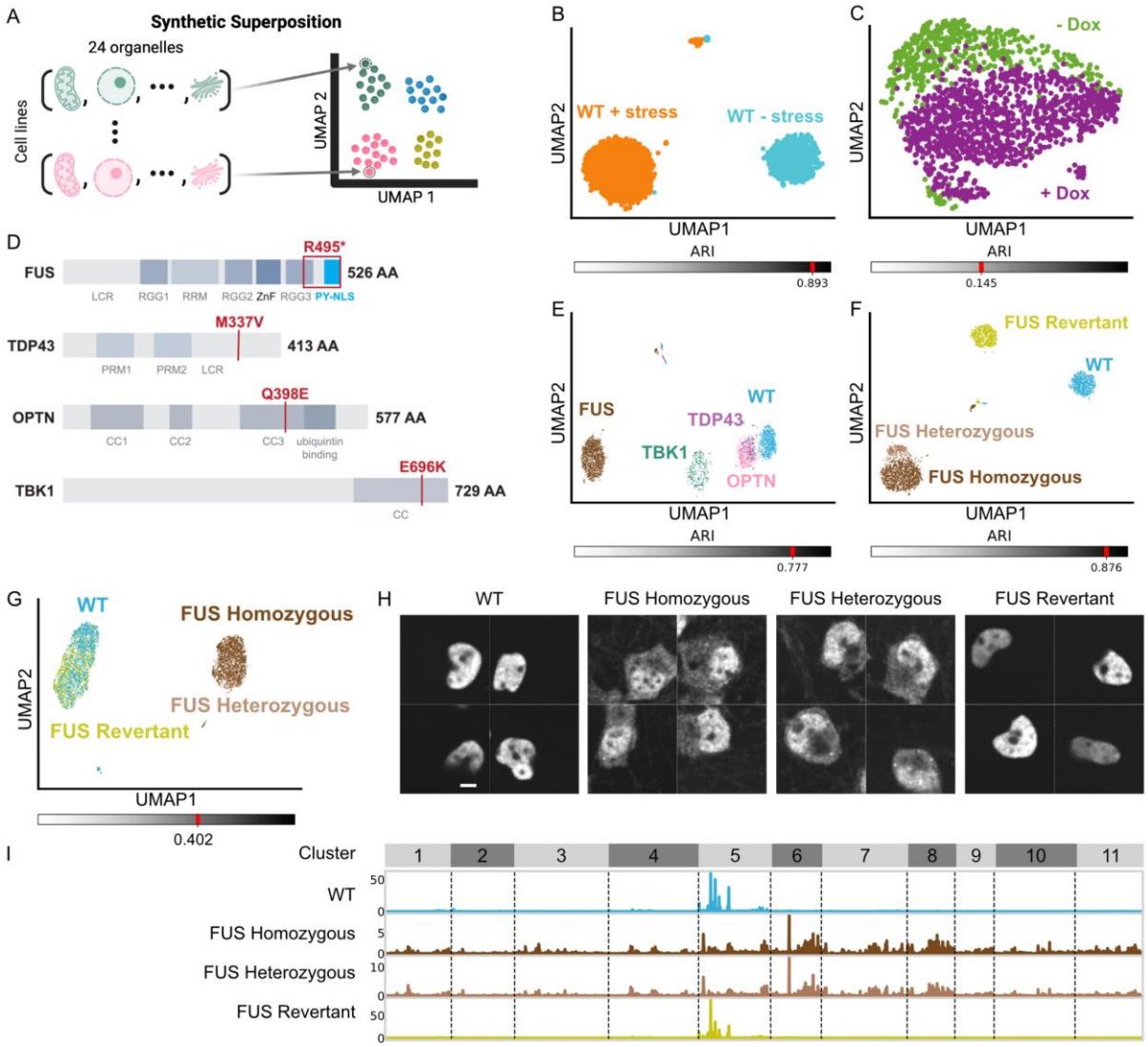

Figure 5: Integrated Organellome Characterization of iNDI ALS Cell Lines. (A) illustrative scheme of the integrated organellome gained by synthetic superposition of all 24 organelles. **(B)** Superposition of ±stress conditions (data from **Figure 3,** ARI = 0.893) and of **(C)** induced and uninduced cytoplasmic TDP-43 conditions (data and model from **Figure 4,** ARI = 0.145). **(D)** Genetic diagram of selected neurodegenerative (iNDI) cell lines harboring ALS-associated mutations. **(E-F)** UMAP of synthetic superposition of 24 organelles in **(E)** wild-type and four genetically different ALS lines (ARI = 0.777) or in **(F)** FUS 495* homozygous, heterozygous, and revertant (corrected) and wild-type lines (ARI = 0.876). **(G)** Single organelle UMAP display of the hnRNP complex (FUS marker) topography of wild-type and FUS lines described in (F), and **(H)** images of the hnRNP complex (FUS marker), scale bar 5µm. **(I)** Feature spectra of the hnRNP complex in WT, FUS homozygous, FUS heterozygous and FUS revertant cell lines.

Discussion

In this work we present NOVA, an AI-driven approach for organellomic studies in neurons. We employ deep variational autoencoder architecture, in a self-supervised strategy, to systematically encode subcellular localization and morphology patterns from immunofluorescent images of 24 membrane-bound and membrane-less organelles. NOVA provides an unprecedented depth to organellar microscopic studies and an integrative view of cell biology.

We leveraged the Cytoself model that was trained on the OpenCell dataset. We applied transfer learning to achieve NOVA's capability to study cultured human neurons, which pose several strengths: first, gaining the knowledge captured from learning localization of 1,311 proteins, which promotes the improved performance of NOVA compared to training a model from scratch. Second, it significantly reduces the time and resources needed for training. Additionally, NOVA can be the foundational baseline for transfer learning in additional AI neurobiology studies, which minimizes the volume of images required for subsequent inquiries. Moreover, our dataset, composed of myriads of neuron microscopic images, is a valuable resource for further investigations.

NOVA does not require cell segmentation, which simplifies data processing and is particularly advantageous when examining highly polarized cells such as neurons.

Importantly, the NOVA Synthetic Superposition method provides a unique way to study the whole integrated organellome. Being performed *in silico*, therefore, NOVA is not limited by the relatively small number of channels that standard light scopes are equipped with. Instead, NOVA relies on simple confocal images, thus providing an inexpensive alternative to cumbersome multiplexing technologies such as CODEX or 4i (Black et al. 2021; Gut, Herrmann, and Pelkmans 2018). Noteworthy, synthetic superposition can be applied to existing microscopy datasets, without setting a limit to the number of organelles.

Methods that generate self-explainable manual engineered features (intensity, shape, granularity, size for a given object), such as CellPainting and CellProfiler (Bray et al. 2016; Stirling et al. 2021), are widely used. However, some markers are not easily demarcated by defined objects. NOVA utilizes deep representation learning, which is unbiased and does not require a pre-defined object or task, hence can describe any localization pattern in the image. Computer vision studies have demonstrated that as compared with the hand-crafted features, the multi-scale features automatically learned by a deep learning model can capture and generalize better (Singh et al. 2020; Caicedo et al. 2017; Sun, Tárnok, and Su 2020; Lavitt et al. 2021). Moreover, NOVA's hierarchical latent spaces enable encoding complex structures and provide potent representations at various (global and local) abstraction levels.

Importantly, this fast and easily implementable approach can be applied retroactively to existing microscopy images, without restricting the number of markers examined in a single analysis. The ease and cost-effectiveness of synthetic superpositioning, leveraging standard confocal microscopes, empower users with access to such instruments to effortlessly capture images and evaluate them using NOVA.

The relevance of organellomics studies root from the intricate network of organellar interactions, which allows cells to regulate compartment content and functions (Cohen, Valm, and Lippincott-

Schwartz 2018; Donahue, Ruark, and Burkewitz 2022; Rossini, Pizzo, and Filadi 2021; Schrader, Kamoshita, and Islinger 2020). This is not limited to membrane-bound organelles, as the intricate cellular communication network extends to encompass interactions of membrane-bound and membraneless organelles (Bussi et al. 2023; Amen and Kaganovich 2021; Liao et al. 2019; Qin et al. 2023) and between different membraneless organelles (Stoecklin and Kedersha 2013). The dynamic interplay within the cellular landscape is accordingly revealed also by the compound multi-organellar dysfunction in disease conditions, e.g., lysosome-peroxisome dysregulation in peroxisomal disorders, (Chu et al. 2015) or mitochondrial dysfunction in lysosomal storage disorders (Plotegher and Duchen 2017).

Our image-based organellomics approach provides a compelling alternative to traditional biochemical methods of organellar fractionation (Itzhak et al. 2017; Borner 2020; Schessner et al. 2023; Itzhak, Schessner, and Borner 2019; Thul et al. 2017), addressing the inherent difficulties of organelle fractionation, particularly in attempting the isolation of liquid-like membraneless organelles (Mitrea et al. 2018).

The NOVA model enables the assessment of how individual organelles respond to perturbations through organelle scoring. This method facilitates direct comparisons across all organelles and provides a way to prioritize them for further studies. Moreover, by capturing the responses of all organelles, it unravels the complete cellular response in a manner previously unachievable, paving the way for evaluating organellar coordination and potential interdependencies.

We demonstrate the utility of NOVA via the study of neuronal response to oxidative stress. The observed expected changes in stress granules were accompanied by the response of several other organelles to stress that had been previously overlooked. Thus, stress triggers a coordinated response involving not just stress granules, but also the mitochondrial outer membrane, lysosomes, and the Golgi apparatus. The hypothesized interaction between the mitochondrial outer membrane and stress granules was further experimentally validated and visualized. We also induced cytoplasmic TDP-43, which is a model of ALS (Tziortzouda, Van Den Bosch, and Hirth 2021). In our study, the significant alteration in P-body topography was the most clear change associated with cytoplasmic localization of TDP-43. Therefore, the interaction of TDP-43 granules and P-bodies might be an important facet of biology. Intriguingly, TDP-43 to P-bodies interactions may be largely independent of stress granules, which did not change in response to the expression of TDP-43 (Lee et al. 2021; I.-F. Wang et al. 2008; Liu-Yesucevitz et al. 2010; Gasset-Rosa et al. 2019).

A key achievement of our study is the integrated organellome approach for cellular states, which is performed by superimposing the topographic information of multiple or even all organelles. We demonstrate the utility of the integrated organellome in a study of several ALS-associated genetic models and focus primarily on FUS R495* neurons that display the most pronounced organellar changes relative to wild-type controls. FUS R495* is deficient of the nuclear localization signal and is clinically associated with an aggressive, juvenile, form of ALS (Waibel et al. 2010). The changes to FUS R495* homozygous and heterozygous organellomes were extremely similar, suggesting that a single mutated allele is sufficient to drive the observed phenotype. Additionally, the cytoplasmic mislocalization of the hnRNP (FUS) complex is recovered in a revertant FUS line. However, the organellome of the FUS revertant line is not fully restored and seems to exhibit some disruptions

relative to the wild-type organellome. Such partial organellar dysregulation might be due to passage in culture or CRISPR off targets.

We cultured iPSC-derived cortical neurons for 8 days. Therefore these neurons are still rather premature. It is plausible that extended culture age or chronic stress will result in additional phenotypes. In this context, it is not clear if the cytoplasmic malposition of the hnRNP (FUS) complex is an early manifestation and whether additional organelle topographies would change with longer culturing time in the FUS R495* model or in any of the other ALS-associated genetic models. We also acknowledge that while the lack of segmentation makes NOVA very efficient, it is limited to studies in homogenous cultures. Further development of segmentation in NOVA might allow for the study of co-cultures, multiple genotypes or even tissue sections. Finally, the model is currently applicable to iPSC-derived cortical neurons. We expect that the model can be fine-tuned and generalized to other disease-relevant cell types. However this will require additional data collection and transfer learning steps.

In summary, organellomics is a novel approach to understanding cellular biology. It can be extended to additional disease phenotypes, to other types of patient-derived cells and to existing image data. Organellomics will likely contribute additional insights to the mechanisms of neuronal diseases and to the generation of novel hypotheses that can be experimentally tested. We suggest that the value of organellomics for genotype-phenotype mapping can broadly impact cellular biology and disease biology research and foster precision medicine for neuronal diseases.

References

Alberti, Simon, and Dorothee Dormann. 2019. “Liquid-Liquid Phase Separation in Disease.” *Annual Review of Genetics* 53 (December): 171–94.

Alberti, Simon, and Anthony A. Hyman. 2021. “Biomolecular Condensates at the Nexus of Cellular Stress, Protein Aggregation Disease and Ageing.” *Nature Reviews. Molecular Cell Biology* 22 (3): 196–213.

Amen, Triana, and Daniel Kaganovich. 2021. “Stress Granules Inhibit Fatty Acid Oxidation by Modulating Mitochondrial Permeability.” *Cell Reports* 35 (11): 109237.

Anderson, Paul, and Nancy Kedersha. 2009. “RNA Granules: Post-Transcriptional and Epigenetic Modulators of Gene Expression.” *Nature Reviews. Molecular Cell Biology* 10 (6): 430–36.

Ascoli, Giorgio A., Duncan E. Donohue, and Maryam Halavi. 2007. “NeuroMorpho.Org: A Central Resource for Neuronal Morphologies.” *The Journal of Neuroscience: The Official Journal of the Society for Neuroscience* 27 (35): 9247–51.

Banani, Salman F., Hyun O. Lee, Anthony A. Hyman, and Michael K. Rosen. 2017. “Biomolecular Condensates: Organizers of Cellular Biochemistry.” *Nature Reviews. Molecular Cell Biology* 18 (5): 285–98.

Bayer, T. A., P. Jäkälä, T. Hartmann, R. Egensperger, R. Buslei, P. Falkai, and K. Beyreuther. 1999. “Neural Expression Profile of Alpha-Synuclein in Developing Human Cortex.” *Neuroreport* 10 (13): 2799–2803.

Bilican, Bilada, Andrea Serio, Sami J. Barmada, Agnes Lumi Nishimura, Gareth J. Sullivan, Monica Carrasco, Hemali P. Phatnani, et al. 2012. “Mutant Induced Pluripotent Stem Cell Lines Recapitulate Aspects of TDP-43 Proteinopathies and Reveal Cell-Specific Vulnerability.” *Proceedings of the National Academy of Sciences*. https://doi.org/10.1073/pnas.1202922109.

Black, Sarah, Darci Phillips, John W. Hickey, Julia Kennedy-Darling, Vishal G. Venkataraaman, Nikolay Samusik, Yury Goltsev, Christian M. Schürch, and Garry P. Nolan. 2021. “CODEX Multiplexed Tissue Imaging with DNA-Conjugated Antibodies.” *Nature Protocols* 16 (8): 3802–35.

Borner, Georg H. H. 2020. “Organellar Maps Through Proteomic Profiling - A Conceptual Guide.” *Molecular & Cellular Proteomics: MCP* 19 (7): 1076–87.

Bozinovski, Stevo. 2020. “Reminder of the First Paper on Transfer Learning in Neural Networks, 1976.” *Lithuanian Academy of Sciences. Informatica* 44 (3). https://doi.org/10.31449/inf.v44i3.2828.

Bradley, P. S., K. P. Bennett, and A. Demiriz. 2000. “Constrained K-Means Clustering.” machinelearning102.pbworks.com. 2000. http://machinelearning102.pbworks.com/f/ConstrainedKMeanstr-2000-65.pdf.

Brangwynne, Clifford P. 2013. “Phase Transitions and Size Scaling of Membrane-Less Organelles.” *The Journal of Cell Biology* 203 (6): 875–81.

Bray, Mark-Anthony, Shantanu Singh, Han Han, Chadwick T. Davis, Blake Borgeson, Cathy Hartland, Maria Kost-Alimova, Sigrun M. Gustafsdottir, Christopher C. Gibson, and Anne E. Carpenter. 2016. “Cell Painting, a High-Content Image-Based Assay for Morphological Profiling Using Multiplexed Fluorescent Dyes.” *Nature Protocols* 11 (9): 1757–74.

Brenner, J. F., B. S. Dew, J. B. Horton, T. King, P. W. Neurath, and W. D. Selles. 1976. “An Automated Microscope for Cytologic Research a Preliminary Evaluation.” *The Journal of Histochemistry and Cytochemistry: Official Journal of the Histochemistry Society* 24 (1): 100–111.

Bussi, Claudio, Agustín Mangiarotti, Christian Vanhille-Campos, Beren Aylan, Enrica Pellegrino, Natalia Athanasiadi, Antony Fearns, et al. 2023. “Stress Granules Plug and Stabilize Damaged Endolysosomal Membranes.” *Nature* 623 (7989): 1062–69.

Caicedo, Juan C., Sam Cooper, Florian Heigwer, Scott Warchal, Peng Qiu, Csaba Molnar, Aliaksei S. Vasilevich, et al. 2017. “Data-Analysis Strategies for Image-Based Cell Profiling.” *Nature Methods* 14 (9): 849–63.

Calvio, C., G. Neubauer, M. Mann, and A. I. Lamond. 1995. “Identification of hnRNP P2 as TLS/FUS

Using Electrospray Mass Spectrometry." *RNA* 1 (7): 724–33.
Carpenter, Anne E., Thouis R. Jones, Michael R. Lamprecht, Colin Clarke, In Han Kang, Ola Friman, David A. Guertin, et al. 2006. "CellProfiler: Image Analysis Software for Identifying and Quantifying Cell Phenotypes." *Genome Biology* 7 (10): R100.
Chazotte, Brad. 2010. "Labeling Cytoskeletal F-Actin with Rhodamine Phalloidin or Fluorescein Phalloidin for Imaging." *Cold Spring Harbor Protocols* 2010 (5): db.prot4947.
———. 2011a. "Labeling Nuclear DNA with Hoechst 33342." *Cold Spring Harbor Protocols* 2011 (1): db.prot5557.
———. 2011b. "Labeling Mitochondria with MitoTracker Dyes." *Cold Spring Harbor Protocols* 2011 (8): 990–92.
Cho, Nathan H., Keith C. Cheveralls, Andreas-David Brunner, Kibeom Kim, André C. Michaelis, Preethi Raghavan, Hirofumi Kobayashi, et al. 2022. "OpenCell: Endogenous Tagging for the Cartography of Human Cellular Organization." *Science* 375 (6585): eabi6983.
Chu, Bei-Bei, Ya-Cheng Liao, Wei Qi, Chang Xie, Ximing Du, Jiang Wang, Hongyuan Yang, Hong-Hua Miao, Bo-Liang Li, and Bao-Liang Song. 2015. "Cholesterol Transport through Lysosome-Peroxisome Membrane Contacts." *Cell* 161 (2): 291–306.
Cohen, Sarah, Alex M. Valm, and Jennifer Lippincott-Schwartz. 2018. "Interacting Organelles." *Current Opinion in Cell Biology* 53 (August): 84–91.
Cox, Timothy M., and M. Begoña Cachón-González. 2012. "The Cellular Pathology of Lysosomal Diseases." *The Journal of Pathology* 226 (2): 241–54.
Daigle, J. Gavin, Karthik Krishnamurthy, Nandini Ramesh, Ian Casci, John Monaghan, Kevin McAvoy, Earl W. Godfrey, et al. 2016. "Pur-Alpha Regulates Cytoplasmic Stress Granule Dynamics and Ameliorates FUS Toxicity." *Acta Neuropathologica* 131 (4): 605–20.
Di Salvio, M., V. Piccinni, V. Gerbino, F. Mantoni, S. Camerini, J. Lenzi, A. Rosa, et al. 2015. "Pur-Alpha Functionally Interacts with FUS Carrying ALS-Associated Mutations." *Cell Death & Disease* 6 (10): e1943.
Donahue, Eric K. F., Elizabeth M. Ruark, and Kristopher Burkewitz. 2022. "Fundamental Roles for Inter-Organelle Communication in Aging." *Biochemical Society Transactions* 50 (5): 1389–1402.
Dormann, Dorothee, Ramona Rodde, Dieter Edbauer, Eva Bentmann, Ingeborg Fischer, Alexander Hruscha, Manuel E. Than, et al. 2010. "ALS-Associated Fused in Sarcoma (FUS) Mutations Disrupt Transportin-Mediated Nuclear Import." *The EMBO Journal* 29 (16): 2841–57.
Du, Mingjian, Chee-Kwee Ea, Yan Fang, and Zhijian J. Chen. 2022. "Liquid Phase Separation of NEMO Induced by Polyubiquitin Chains Activates NF-κB." *Molecular Cell* 82 (13): 2415–26.e5.
Eystathioy, Theophany, Andrew Jakymiw, Edward K. L. Chan, Bertrand Séraphin, Nicolas Cougot, and Marvin J. Fritzler. 2003. "The GW182 Protein Colocalizes with mRNA Degradation Associated Proteins hDcp1 and hLSm4 in Cytoplasmic GW Bodies." *RNA* 9 (10): 1171–73.
Feneberg, Emily, David Gordon, Alexander G. Thompson, Mattéa J. Finelli, Ruxandra Dafinca, Ana Candalija, Philip D. Charles, et al. 2020. "An ALS-Linked Mutation in TDP-43 Disrupts Normal Protein Interactions in the Motor Neuron Response to Oxidative Stress." *Neurobiology of Disease* 144 (October): 105050.
Fernandopulle, Michael S., Ryan Prestil, Christopher Grunseich, Chao Wang, Li Gan, and Michael E. Ward. 2018. "Transcription Factor-Mediated Differentiation of Human iPSCs into Neurons." *Current Protocols in Cell Biology / Editorial Board, Juan S. Bonifacino ... [et Al.]* 79 (1): e51.
Fox, Archa H., Charles S. Bond, and Angus I. Lamond. 2005. "P54nrb Forms a Heterodimer with PSP1 That Localizes to Paraspeckles in an RNA-Dependent Manner." *Molecular Biology of the Cell* 16 (11): 5304–15.
Fox, Archa H., Yun Wah Lam, Anthony K. L. Leung, Carol E. Lyon, Jens Andersen, Matthias Mann, and Angus I. Lamond. 2002. "Paraspeckles: A Novel Nuclear Domain." *Current Biology: CB* 12 (1): 13–25.
Gasset-Rosa, Fatima, Shan Lu, Haiyang Yu, Cong Chen, Ze 'ev Melamed, Lin Guo, James Shorter, Sandrine Da Cruz, and Don W. Cleveland. 2019. "Cytoplasmic TDP-43 De-Mixing Independent of

Stress Granules Drives Inhibition of Nuclear Import, Loss of Nuclear TDP-43, and Cell Death." *Neuron* 102 (2): 339–57.e7.

Gorman, Gráinne S., Patrick F. Chinnery, Salvatore DiMauro, Michio Hirano, Yasutoshi Koga, Robert McFarland, Anu Suomalainen, David R. Thorburn, Massimo Zeviani, and Douglass M. Turnbull. 2016. "Mitochondrial Diseases." *Nature Reviews. Disease Primers* 2 (October): 16080.

Gottschling, Daniel E., and Thomas Nyström. 2017. "The Upsides and Downsides of Organelle Interconnectivity." *Cell* 169 (1): 24–34.

Gowrishankar, Swetha, Yumei Wu, and Shawn M. Ferguson. 2017. "Impaired JIP3-Dependent Axonal Lysosome Transport Promotes Amyloid Plaque Pathology." *The Journal of Cell Biology* 216 (10): 3291–3305.

Gut, G., Herrmann, and L. Pelkmans. 2018. "Multiplexed Protein Maps Link Subcellular Organization to Cellular States." *Science* 361 (6401). https://doi.org/10.1126/science.aar7042.

Heinrich, Larissa, Davis Bennett, David Ackerman, Woohyun Park, John Bogovic, Nils Eckstein, Alyson Petruncio, et al. 2021. "Whole-Cell Organelle Segmentation in Volume Electron Microscopy." *Nature* 599 (7883): 141–46.

Hirose, Tetsuro, Kensuke Ninomiya, Shinichi Nakagawa, and Tomohiro Yamazaki. 2022. "A Guide to Membraneless Organelles and Their Various Roles in Gene Regulation." *Nature Reviews. Molecular Cell Biology*, November. https://doi.org/10.1038/s41580-022-00558-8.

Hofweber, Mario, Saskia Hutten, Benjamin Bourgeois, Emil Spreitzer, Annika Niedner-Boblenz, Martina Schifferer, Marc-David Ruepp, et al. 2018. "Phase Separation of FUS Is Suppressed by Its Nuclear Import Receptor and Arginine Methylation." *Cell* 173 (3): 706–19.e13.

Husain, Syed Sameed, Eng-Jon Ong, Dmitry Minskiy, Mikel Bober-Irizar, Amaia Irizar, and Miroslaw Bober. 2023. "Single-Cell Subcellular Protein Localisation Using Novel Ensembles of Diverse Deep Architectures." *Communications Biology* 6 (1): 489.

Itzhak, Daniel N., Colin Davies, Stefka Tyanova, Archana Mishra, James Williamson, Robin Antrobus, Jürgen Cox, Michael P. Weekes, and Georg H. H. Borner. 2017. "A Mass Spectrometry-Based Approach for Mapping Protein Subcellular Localization Reveals the Spatial Proteome of Mouse Primary Neurons." *Cell Reports* 20 (11): 2706–18.

Itzhak, Daniel N., Julia P. Schessner, and Georg H. H. Borner. 2019. "Dynamic Organellar Maps for Spatial Proteomics." *Current Protocols in Cell Biology / Editorial Board, Juan S. Bonifacino ... [et Al.]* 83 (1): e81.

Kageyama, Shun, Sigurdur Runar Gudmundsson, Yu-Shin Sou, Yoshinobu Ichimura, Naoki Tamura, Saiko Kazuno, Takashi Ueno, et al. 2021. "p62/SQSTM1-Droplet Serves as a Platform for Autophagosome Formation and Anti-Oxidative Stress Response." *Nature Communications* 12 (1): 16.

Kim, Kwang-Min, Kilho Son, and G. Tayhas R. Palmore. 2015. "Neuron Image Analyzer: Automated and Accurate Extraction of Neuronal Data from Low Quality Images." *Scientific Reports* 5 (November): 17062.

Kobayashi, Hirofumi, Keith C. Cheveralls, Manuel D. Leonetti, and Loic A. Royer. 2022. "Self-Supervised Deep Learning Encodes High-Resolution Features of Protein Subcellular Localization." *Nature Methods* 19 (8): 995–1003.

Koyano, Fumika, Koji Yamano, Hidetaka Kosako, Yoko Kimura, Mayumi Kimura, Yukio Fujiki, Keiji Tanaka, and Noriyuki Matsuda. 2019. "Parkin-Mediated Ubiquitylation Redistributes MITOL/March5 from Mitochondria to Peroxisomes." *EMBO Reports* 20 (12): e47728.

Lavitt, Falko, Demi J. Rijlaarsdam, Dennet van der Linden, Ewelina Weglarz-Tomczak, and Jakub M. Tomczak. 2021. "Deep Learning and Transfer Learning for Automatic Cell Counting in Microscope Images of Human Cancer Cell Lines." *APPS. Applied Sciences* 11 (11): 4912.

Lee, Youn-Bok, Emma L. Scotter, Do-Young Lee, Claire Troakes, Jacqueline Mitchell, Boris Rogelj, Jean-Marc Gallo, and Christopher E. Shaw. 2021. "Cytoplasmic TDP-43 Is Involved in Cell Fate during Stress Recovery." *Human Molecular Genetics* 31 (2): 166–75.

Levine, Beth, and Guido Kroemer. 2008. "Autophagy in the Pathogenesis of Disease." *Cell* 132 (1):

638 27–42.
639 Liao, Ya-Cheng, Michael S. Fernandopulle, Guozhen Wang, Heejun Choi, Ling Hao, Catherine M.
640 Drerup, Rajan Patel, et al. 2019. "RNA Granules Hitchhike on Lysosomes for Long-Distance
641 Transport, Using Annexin A11 as a Molecular Tether." *Cell* 179 (1): 147–64.e20.
642 Li, Faxiang, Xingqiao Xie, Yingli Wang, Jianping Liu, Xiaofang Cheng, Yujiao Guo, Yukang Gong,
643 Shichen Hu, and Lifeng Pan. 2016. "Structural Insights into the Interaction and Disease
644 Mechanism of Neurodegenerative Disease-Associated Optineurin and TBK1 Proteins." *Nature*
645 *Communications* 7 (September): 12708.
646 Liu, Mengyu, Huifeng Pi, Yu Xi, Liting Wang, Li Tian, Mengyan Chen, Jia Xie, et al. 2021. "KIF5A-
647 Dependent Axonal Transport Deficiency Disrupts Autophagic Flux in Trimethyltin Chloride-
648 Induced Neurotoxicity." *Autophagy* 17 (4): 903–24.
649 Liu-Yesucevitz, Liqun, Aylin Bilgutay, Yong-Jie Zhang, Tara Vanderweyde, Allison Citro, Tapan Mehta,
650 Nava Zaarur, et al. 2010. "Tar DNA Binding Protein-43 (TDP-43) Associates with Stress Granules:
651 Analysis of Cultured Cells and Pathological Brain Tissue." *PloS One* 5 (10): e13250.
652 Long, Wei, Yang Yang, and Hong-Bin Shen. 2020. "ImPLoc: A Multi-Instance Deep Learning Model for
653 the Prediction of Protein Subcellular Localization Based on Immunohistochemistry Images."
654 *Bioinformatics* 36 (7): 2244–50.
655 Lu, Alex X., Oren Z. Kraus, Sam Cooper, and Alan M. Moses. 2019. "Learning Unsupervised Feature
656 Representations for Single Cell Microscopy Images with Paired Cell Inpainting." *PLoS*
657 *Computational Biology* 15 (9): e1007348.
658 Lyon, Andrew S., William B. Peeples, and Michael K. Rosen. 2021. "A Framework for Understanding
659 the Functions of Biomolecular Condensates across Scales." *Nature Reviews. Molecular Cell*
660 *Biology* 22 (3): 215–35.
661 Markmiller, Sebastian, Sahar Soltanieh, Kari L. Server, Raymond Mak, Wenhao Jin, Mark Y. Fang, En-
662 Ching Luo, et al. 2018. "Context-Dependent and Disease-Specific Diversity in Protein
663 Interactions within Stress Granules." *Cell* 172 (3): 590–604.e13.
664 Marmor-Kollet, Hagai, Aviad Siany, Nancy Kedersha, Naama Knafo, Natalia Rivkin, Yehuda M.
665 Danino, Thomas G. Moens, et al. 2020. "Spatiotemporal Proteomic Analysis of Stress Granule
666 Disassembly Using APEX Reveals Regulation by SUMOylation and Links to ALS Pathogenesis."
667 *Molecular Cell* 80 (5): 876–91.e6.
668 Mitrea, Diana M., Bappaditya Chandra, Mylene C. Ferrolino, Eric B. Gibbs, Michele Tolbert, Michael
669 R. White, and Richard W. Kriwacki. 2018. "Methods for Physical Characterization of Phase-
670 Separated Bodies and Membrane-Less Organelles." *Journal of Molecular Biology* 430 (23):
671 4773–4805.
672 Mizushima, Noboru, and Beth Levine. 2020. "Autophagy in Human Diseases." *The New England*
673 *Journal of Medicine* 383 (16): 1564–76.
674 Mobarrez, Fariborz, Anna Vikerfors, Johanna T. Gustafsson, Iva Gunnarsson, Agneta Zickert, Anders
675 Larsson, David S. Pisetsky, Håkan Wallén, and Elisabet Svenungsson. 2016. "Microparticles in
676 the Blood of Patients with Systemic Lupus Erythematosus (SLE): Phenotypic Characterization
677 and Clinical Associations." *Scientific Reports* 6 (October): 36025.
678 Molitor, Lena, Melina Klostermann, Sabrina Bacher, Juliane Merl-Pham, Nadine Spranger, Sandra
679 Burczyk, Carolin Ketteler, et al. 2023. "Depletion of the RNA-Binding Protein PURA Triggers
680 Changes in Posttranscriptional Gene Regulation and Loss of P-Bodies." *Nucleic Acids Research*
681 51 (3): 1297–1316.
682 Mutihac, R., J. Alegre-Abarrategui, D. Gordon, L. Farrimond, M. Yamasaki-Mann, K. Talbot, and R.
683 Wade-Martins. 2015. "TARDBP Pathogenic Mutations Increase Cytoplasmic Translocation of
684 TDP-43 and Cause Reduction of Endoplasmic Reticulum Ca^{2+} Signaling in Motor Neurons."
685 *Neurobiology of Disease* 75 (March): 64–77.
686 Naganuma, Takao, Shinichi Nakagawa, Akie Tanigawa, Yasnory F. Sasaki, Naoki Goshima, and Tetsuro
687 Hirose. 2012. "Alternative 3'-End Processing of Long Noncoding RNA Initiates Construction of
688 Nuclear Paraspeckles." *The EMBO Journal* 31 (20): 4020–34.

Nava, Caroline, Johanna Rupp, Jean-Paul Boissel, Cyril Mignot, Agnès Rastetter, Claire Amiet, Aurélia Jacquette, et al. 2015. “Hypomorphic Variants of Cationic Amino Acid Transporter 3 in Males with Autism Spectrum Disorders.” *Amino Acids* 47 (12): 2647–58.

Nedelsky, Natalia B., and J. Paul Taylor. 2019. “Bridging Biophysics and Neurology: Aberrant Phase Transitions in Neurodegenerative Disease.” *Nature Reviews. Neurology* 15 (5): 272–86.

Oberlaender, Marcel, Randy M. Bruno, Bert Sakmann, and Philip J. Broser. 2007. “Transmitted Light Brightfield Mosaic Microscopy for Three-Dimensional Tracing of Single Neuron Morphology.” *Journal of Biomedical Optics* 12 (6): 064029.

Oord, Aaron van den, Oriol Vinyals, and Koray Kavukcuoglu. 2017. “Neural Discrete Representation Learning.” https://doi.org/10.48550/ARXIV.1711.00937.

Pantazis, Caroline B., Andrian Yang, Erika Lara, Justin A. McDonough, Cornelis Blauwendraat, Lirong Peng, Hideyuki Oguro, et al. 2022. “A Reference Human Induced Pluripotent Stem Cell Line for Large-Scale Collaborative Studies.” *Cell Stem Cell* 29 (12): 1685–1702.e22.

Paszke, Adam, Sam Gross, Francisco Massa, Adam Lerer, James Bradbury, Gregory Chanan, Trevor Killeen, et al. 2019. “Pytorch: An Imperative Style, High-Performance Deep Learning Library.” *Advances in Neural Information Processing Systems* 32. https://proceedings.neurips.cc/paper_files/paper/2019/hash/bdbca288fee7f92f2bfa9f7012727740-Abstract.html.

Platt, Frances M., Alessandra d’Azzo, Beverly L. Davidson, Elizabeth F. Neufeld, and Cynthia J. Tifft. 2018. “Lysosomal Storage Diseases.” *Nature Reviews. Disease Primers* 4 (1): 27.

Plotegher, Nicoletta, and Michael R. Duchen. 2017. “Mitochondrial Dysfunction and Neurodegeneration in Lysosomal Storage Disorders.” *Trends in Molecular Medicine* 23 (2): 116–34.

Protter, David S. W., and Roy Parker. 2016. “Principles and Properties of Stress Granules.” *Trends in Cell Biology* 26 (9): 668–79.

Qin, Wei, Joleen S. Cheah, Charles Xu, James Messing, Brian D. Freibaum, Steven Boeynaems, J. Paul Taylor, Namrata D. Udeshi, Steven A. Carr, and Alice Y. Ting. 2023. “Dynamic Mapping of Proteome Trafficking within and between Living Cells by TransitID.” *Cell* 186 (15): 3307–24.e30.

Qiu, Yueping, Jincheng Wang, Hui Li, Bo Yang, Jiajia Wang, Qiaojun He, and Qinjie Weng. 2022. “Emerging Views of OPTN (optineurin) Function in the Autophagic Process Associated with Disease.” *Autophagy* 18 (1): 73–85.

Ramos, Daniel M., William C. Skarnes, Andrew B. Singleton, Mark R. Cookson, and Michael E. Ward. 2021. “Tackling Neurodegenerative Diseases with Genomic Engineering: A New Stem Cell Initiative from the NIH.” *Neuron* 109 (7): 1080–83.

Ray, Soumik, Nitu Singh, Rakesh Kumar, Komal Patel, Satyaprakash Pandey, Debalina Datta, Jaladhar Mahato, et al. 2020. “α-Synuclein Aggregation Nucleates through Liquid-Liquid Phase Separation.” *Nature Chemistry* 12 (8): 705–16.

Razavi, Ali, Aaron van den Oord, and Oriol Vinyals. 2019. “Generating Diverse High-Fidelity Images with VQ-VAE-2.” https://doi.org/10.48550/ARXIV.1906.00446.

Rossini, Michela, Paola Pizzo, and Riccardo Filadi. 2021. “Better to Keep in Touch: Investigating Inter-Organelle Cross-Talk.” *The FEBS Journal* 288 (3): 740–55.

Sampedro, M. N., C. M. Bussineau, and C. W. Cotman. 1981. “Postsynaptic Density Antigens: Preparation and Characterization of an Antiserum against Postsynaptic Densities.” *The Journal of Cell Biology* 90 (3): 675–86.

Schapira, Anthony H. V. 2006. “Mitochondrial Disease.” *The Lancet* 368 (9529): 70–82.

Schessner, Julia P., Vincent Albrecht, Alexandra K. Davies, Pavel Sinitcyn, and Georg H. H. Borner. 2023. “Deep and Fast Label-Free Dynamic Organellar Mapping.” *Nature Communications* 14 (1): 5252.

Schrader, Michael, Maki Kamoshita, and Markus Islinger. 2020. “Organelle Interplay-Peroxisome Interactions in Health and Disease.” *Journal of Inherited Metabolic Disease* 43 (1): 71–89.

Shelkovnikova, Tatyana A., Hannah K. Robinson, Claire Troakes, Natalia Ninkina, and Vladimir L.

Buchman. 2014. “Compromised Paraspeckle Formation as a Pathogenic Factor in FUSopathies.” *Human Molecular Genetics* 23 (9): 2298–2312.

Singh, Satya P., Lipo Wang, Sukrit Gupta, Haveesh Goli, Parasuraman Padmanabhan, and Balázs Gulyás. 2020. “3D Deep Learning on Medical Images: A Review.” *Sensors* 20 (18). https://doi.org/10.3390/s20185097.

Spitzer, Hannah, Scott Berry, Mark Donoghoe, Lucas Pelkmans, and Fabian J. Theis. 2023. “Learning Consistent Subcellular Landmarks to Quantify Changes in Multiplexed Protein Maps.” *Nature Methods* 20 (7): 1058–69.

Srivastava, M., P. J. Fleming, H. B. Pollard, and A. L. Burns. 1989. “Cloning and Sequencing of the Human Nucleolin cDNA.” *FEBS Letters* 250 (1): 99–105.

Stirling, David R., Madison J. Swain-Bowden, Alice M. Lucas, Anne E. Carpenter, Beth A. Cimini, and Allen Goodman. 2021. “CellProfiler 4: Improvements in Speed, Utility and Usability.” *BMC Bioinformatics* 22 (1): 433.

Stoecklin, Georg, and Nancy Kedersha. 2013. “Relationship of GW/P-Bodies with Stress Granules.” *Advances in Experimental Medicine and Biology* 768: 197–211.

Stringer, Carsen, Tim Wang, Michalis Michaelos, and Marius Pachitariu. 2021. “Cellpose: A Generalist Algorithm for Cellular Segmentation.” *Nature Methods* 18 (1): 100–106.

Sun, Jing, Attila Tárnok, and Xuantao Su. 2020. “Deep Learning-Based Single-Cell Optical Image Studies.” *Cytometry. Part A: The Journal of the International Society for Analytical Cytology* 97 (3): 226–40.

Thul, Peter J., Lovisa Åkesson, Mikaela Wiking, Diana Mahdessian, Aikaterini Geladaki, Hammou Ait Blal, Tove Alm, et al. 2017. “A Subcellular Map of the Human Proteome.” *Science* 356 (6340). https://doi.org/10.1126/science.aal3321.

Tourrière, Helene, Karim Chebli, Latifa Zekri, Brice Courselaud, Jean Marie Blanchard, Edouard Bertrand, and Jamal Tazi. 2003. “The RasGAP-Associated Endoribonuclease G3BP Assembles Stress Granules.” *The Journal of Cell Biology* 160 (6): 823–31.

Tsuji, Hiroshi, Takashi Nonaka, Makiko Yamashita, Masami Masuda-Suzukake, Fuyuki Kametani, Haruhiko Akiyama, David M. A. Mann, Akira Tamaoka, and Masato Hasegawa. 2012. “Epitope Mapping of Antibodies against TDP-43 and Detection of Protease-Resistant Fragments of Pathological TDP-43 in Amyotrophic Lateral Sclerosis and Frontotemporal Lobar Degeneration.” *Biochemical and Biophysical Research Communications* 417 (1): 116–21.

Tsygankova, Oxana M., and James H. Keen. 2019. “A Unique Role for Clathrin Light Chain A in Cell Spreading and Migration.” *Journal of Cell Science* 132 (10). https://doi.org/10.1242/jcs.224030.

Turner, Declan L., Denis V. Korneev, John G. Purdy, Alex de Marco, and Rommel A. Mathias. 2020. “The Host Exosome Pathway Underpins Biogenesis of the Human Cytomegalovirus Virion.” *eLife* 9 (September): e58288.

Tziortzouda, Paraskevi, Ludo Van Den Bosch, and Frank Hirth. 2021. “Triad of TDP43 Control in Neurodegeneration: Autoregulation, Localization and Aggregation.” *Nature Reviews. Neuroscience* 22 (4): 197–208.

Waibel, S., M. Neumann, M. Rabe, T. Meyer, and A. C. Ludolph. 2010. “Novel Missense and Truncating Mutations in FUS/TLS in Familial ALS.” *Neurology* 75 (9): 815–17.

Wang, Fengsheng, and Leyi Wei. 2022. “Multi-Scale Deep Learning for the Imbalanced Multi-Label Protein Subcellular Localization Prediction Based on Immunohistochemistry Images.” *Bioinformatics* 38 (9): 2602–11.

Wang, I-Fan, Lien-Szn Wu, Hsiang-Yu Chang, and C-K James Shen. 2008. “TDP-43, the Signature Protein of FTLD-U, Is a Neuronal Activity-Responsive Factor.” *Journal of Neurochemistry* 105 (3): 797–806.

Weis, K., S. Rambaud, C. Lavau, J. Jansen, T. Carvalho, M. Carmo-Fonseca, A. Lamond, and A. Dejean. 1994. “Retinoic Acid Regulates Aberrant Nuclear Localization of PML-RAR Alpha in Acute Promyelocytic Leukemia Cells.” *Cell* 76 (2): 345–56.

West, Jason A., Mari Mito, Satoshi Kurosaka, Toru Takumi, Chiharu Tanegashima, Takeshi Chujo,

Kaori Yanaka, et al. 2016. “Structural, Super-Resolution Microscopy Analysis of Paraspeckle Nuclear Body Organization.” *The Journal of Cell Biology* 214 (7): 817–30.

Wurm, Christian A., Daniel Neumann, Marcel A. Lauterbach, Benjamin Harke, Alexander Egner, Stefan W. Hell, and Stefan Jakobs. 2011. “Nanoscale Distribution of Mitochondrial Import Receptor Tom20 Is Adjusted to Cellular Conditions and Exhibits an Inner-Cellular Gradient.” *Proceedings of the National Academy of Sciences of the United States of America* 108 (33): 13546–51.

Xiang, Qian, Shun-Dong Ji, Zhuo Zhang, Xia Zhao, and Yi-Min Cui. 2016. “Identification of ITGA2B and ITGB3 Single-Nucleotide Polymorphisms and Their Influences on the Platelet Function.” *BioMed Research International* 2016 (November): 5675084.

Yang, Liuqing, Jozsef Gal, Jing Chen, and Haining Zhu. 2014. “Self-Assembled FUS Binds Active Chromatin and Regulates Gene Transcription.” *Proceedings of the National Academy of Sciences of the United States of America* 111 (50): 17809–14.

Yoshizawa, Takuya, Rustam Ali, Jenny Jiou, Ho Yee Joyce Fung, Kathleen A. Burke, Seung Joong Kim, Yuan Lin, et al. 2018. “Nuclear Import Receptor Inhibits Phase Separation of FUS through Binding to Multiple Sites.” *Cell* 173 (3): 693–705.e22.

Zhang, Zhijun, Sandra Almeida, Yubing Lu, Agnes L. Nishimura, Lingtao Peng, Danqiong Sun, Bei Wu, et al. 2013. “Downregulation of MicroRNA-9 in iPSC-Derived Neurons of FTD/ALS Patients with TDP-43 Mutations.” *PLoS ONE*. https://doi.org/10.1371/journal.pone.0076055.

Zung, Naama, and Maya Schuldiner. 2020. “New Horizons in Mitochondrial Contact Site Research.” *Biological Chemistry* 401 (6-7): 793–809.